On the lateral fluid motion during pool boiling via preferentially located cavities

Citation	Kapsenberg, F., Strid, L., Thiagarajan, N., Narayanan, V., & Bhavnani, S. H. (2014). On the lateral fluid motion during pool boiling via preferentially located cavities. Applied Physics Letters, 104(15), 154105. doi:10.1063/1.4871863
DOI	10.1063/1.4871863
Publisher	American Institute of Physics Publishing
Version	Version of Record
Terms of Use	http://cdss.library.oregonstate.edu/sa-termsofuse

On the lateral fluid motion during pool boiling via preferentially located cavities

F. Kapsenberg,[1] L. Strid,[1] N. Thiagarajan,[2] V. Narayanan,[1,a)] and S. H. Bhavnani[2]
[1]*School of Mechanical, Industrial and Manufacturing Engineering, Oregon State University, 204 Rogers Hall, Corvallis, Oregon 97331-6001, USA*
[2]*Department of Mechanical Engineering, Auburn University, Auburn, Alabama 36849, USA*

(Received 11 March 2014; accepted 31 March 2014; published online 17 April 2014)

Passively generated lateral motion of fluid during pool boiling on asymmetrically textured meso-scale structures is discussed in this Letter. The surface texture is in the form of 30°–60° mm-scale ratchets with re-entrant cavities located on the 30° face. High speed visualization of growing bubbles from cavities indicates growth and departure normal to the 30° face of the ratchets. A semi-empirical model of net axial liquid velocity due to the non-vertical bubble growth is developed and validated in a pool boiling experiment. © *2014 AIP Publishing LLC*. [http://dx.doi.org/10.1063/1.4871863]

Surface enhancements for boiling have been studied for several decades from a viewpoint of enhancing heat transfer rate by tailoring nucleation sites (for example, see Refs. 1–6). Here, we explore the possibility to move liquid using enhanced surfaces during pool boiling. Linke *et al.*[7] and other follow-on studies have shown that liquid droplets[8,9] and sublimating solids[10] can be propelled using ratchet like surface asymmetry in the Leidenfrost regime (film boiling). While significant droplet velocities on the order of 50–400 mm/s can be obtained,[7,9] heat transfer rates are generally poor, and surface temperatures high for practical devices such as electronics due to the presence of a vapor film between the surface and the droplet. We wanted to explore whether one could utilize surface asymmetry in microstructure to affect lateral motion of liquid in the *nucleate boiling regime*, wherein the heat transfer rates and coefficients are significantly higher, and surface temperatures significantly lower, than in the Leidenfrost regime.

We employ the same type of asymmetry as that in Linke *et al.*,[7] viz., mm-sized ratchets with shallow (24°–30°) and steep (66°–60°) faces. In addition, we have added reentrant cavities to one (shallow) slope of each ratchet such that an asymmetry exists in the location of cavities (and hence bubbles) on either side of the ratchet (Figs. 1(a) and 1(b)). The microstructured surfaces were created using silicon fabrication methods and are detailed in Thiagarajan *et al.*[11] We hypothesize that, upon supply of sufficient superheat to the surface via addition of heat, bubbles would emanate preferentially from the cavities and grow normal to the sloped ratchet face while being attached to the surface. We further hypothesize that such bubble growth on the ratcheted surfaces will result in liquid motion with a net axial velocity component (Fig. 1(c)). Figures 1(d) and 1(e) and 1(f) and 1(g) show example images from high speed videos of boiling from such structured surfaces using two fluids with distinct properties—water and a dielectric fluorinert, FC-72. The structured surfaces were located in a quiescent pool of the fluid at atmospheric pressure and the pool temperature was controlled to be either close to saturation or subcooled condition using cooling coils. Consistent with the first hypothesis, high speed video images from both experiments indicate growth of the bubble normal to the shallow slope at the cavity location. Detailed growth rate data for FC-72 were determined from high speed videos and image processing over heat fluxes ranging from 0–4.5 W/cm and subcooling ranging from 0 to 20 °C.[12] Over this range of conditions, the initial growth phase was rapid, indicative of an inertially controlled growth regime;[13] while the later stages of growth was slow, indicative of a heat transfer controlled bubble growth. Based on the videos in Fig. 1, it is also clear that the growth of the bubble is non-spherical with coalescence of a growing bubble with a departed bubble in the case of water (Fig. 1(e)).

We now proceed to demonstrate that the non-vertical growth of the bubbles results in a net lateral motion of liquid through a simple force balance model and experiment. Consider a bubble, with a diameter of d_i and height h_i at a time instant i growing at a cavity site as shown in Fig. 2. At a later stage in growth (i + 1), the bubble is indicated as having a diameter d_{i+1} and height h_{i+1}. The growth of the bubble imparts a momentum, $\vec{P}_l = \{\rho_l A_{inf} \vec{v}_l f_d^{-1}\}\vec{v}_l$, to the liquid in a control volume indicated in Fig. 2. The cross-sectional area of the liquid affected by the bubble growth is denoted as A_{inf}, while the height of the control volume is given by a product of the liquid velocity, $\vec{v}_l$, and frequency of bubble departure, f_d. Drag force by the liquid on the bubble impedes the growth rate of the bubble. A momentum balance therefore gives

$$\vec{F}_g = \frac{d\vec{P}_l}{dt} = \frac{d\{\{\rho_l A_{inf} \vec{v}_l f_d^{-1}\}\vec{v}_l\}}{dt} = \frac{1}{8}\pi\rho_l C_D d^2 \left(\frac{\partial \vec{h}}{dt}\right)^2, \quad (1)$$

where the relative velocity between the bubble and the liquid is represented as $\partial\vec{h}/\partial t$. Based on the oblong shape of the bubbles in Fig. 1, bubble height was considered indicative of the interfacial velocity, while the bubble diameter was used for drag force. Equation (1) can provide an analytical expression for determining liquid velocity if the bubble growth rate could be predicted without any empiricism. Traditional models of growth rate for inertially controlled and heat transfer

a)Author to whom correspondence should be addressed. Electronic mail: vinod.narayanan@oregonstate.edu

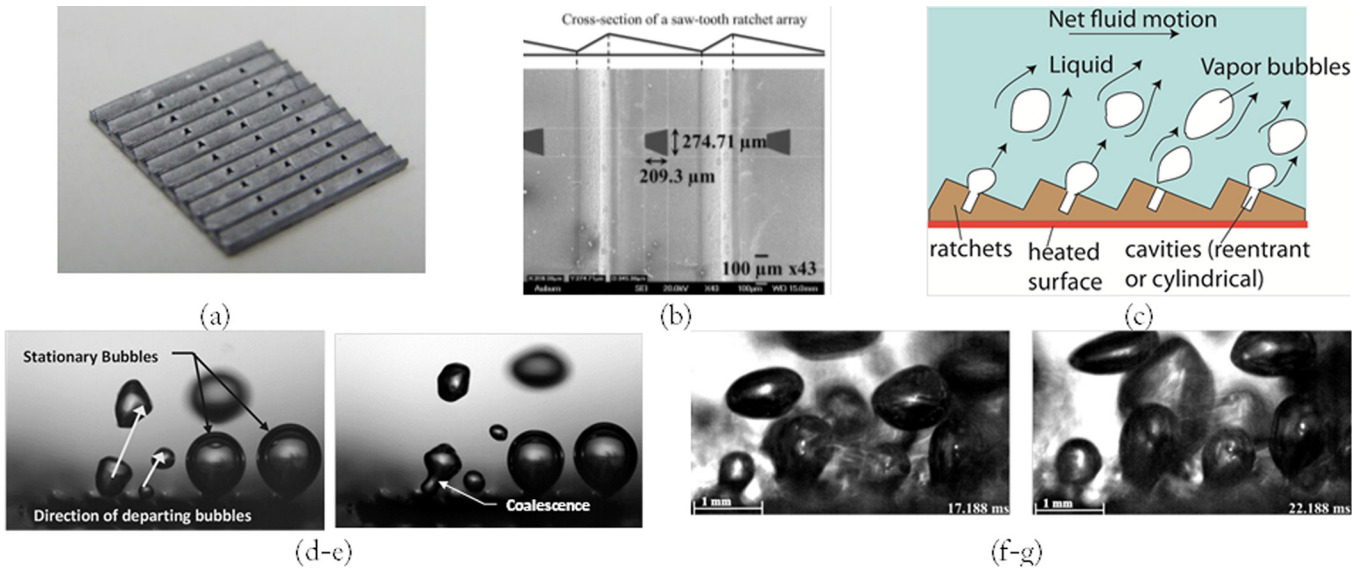

FIG. 1. Growth of bubbles on asymmetrically structured surfaces. (a) Fabricated silicon structured surface with 1-mm pitch ratchets with 24° angle on the shallow face and 24 pyramidal reentrant cavities (details of fabrication are shown in Thiagarajan *et al.*[11]). (b) SEM image showing the top view of saw teeth and cavity mouth measurements. (c) Schematic of the concept illustrating the hypothesis. (d) and (e) Two images, 3.13 ms apart, from a video sequence of a pool boiling experiment with the test surface shown in (a) and deionized degassed water as the working fluid. The applied heat flux, $q''_{applied}$, was 2 ± 0.3 W/cm^2 and the fluid subcooling, ΔT_{sub}, was 4.9 ± 0.3 °C. The field of view was 8.61 mm × 5.38 mm. From Kapsenberg *et al.*, in *Proceedings of 13th IEEE Intersociety Conference on ITherm*. Copyright 2012 IEEE. Reprinted by permission of IEEE.[18] (f) and (g) Two images, 5.0 ms apart, from a video sequence of a pool boiling experiment with the test surface shown in (a) and a fluorinert dielectric FC-72 as the working fluid. The applied heat flux, $q''_{applied}$, was 3.75 ± 0.3 W/cm^2 at saturation condition (zero subcooling). The field of view was 8.61 mm × 5.38 mm. For both video sequences, a Phantom v310 high speed camera with a long working distance objective was used for recording videos with backlit lighting. The videos were recorded at 3200 frames per second with an exposure time of 40 μs. (Multimedia view) [URL: http://dx.doi.org/10.1063/1.4871863.1] [URL: http://dx.doi.org/10.1063/1.4871863.2]

controlled regimes were compared with the growth rate seen in the present experiments.[12] Unlike in typical inertially controlled growth over a flat surface,[13] we did not observe the presence of a liquid microlayer. It is likely that smaller bubbles formed within the reentrant cavity and merged together before being ejected from the cavity as bubbles seen in Fig. 1.

Hence, we resorted to a semi-empirical determination of $\vec{v_l}$ by using growth rate data from high speed videos. Since discrete high-speed images were recorded, Eq. (1) was discretized with a time step corresponding to the interval between two consecutive frames

$$\vec{P_l} = \frac{1}{8}\pi\rho_l \sum_{i=t_0+1}^{t_f} C_D \left(\frac{d_i + d_{i-1}}{2}\right)^2 \left(\frac{h_i + h_{i-1}}{dt}\right)^2 dt. \quad (2)$$

Because the rate of growth of bubble height is determined between two frames, the diameter in Eq. (2) was estimated as the average diameter between the two frames. To determine the drag coefficient C_D in Eq. (2), the Reynolds number based on the average diameter and bubble height growth rate was used. For simplicity, albeit an approximation, values for C_D were determined based on flow over a sphere.[14] The liquid velocity in A_{inf} can be determined by expressing $\vec{P_l}$ in terms of the velocity in Eq. (2)

$$\bar{v}_l = \sqrt{\frac{\pi f_d}{8A_{inf}} \sum_{i=t_0+1}^{t_f} \overline{C_D} \left(\frac{d_i + d_{i-1}}{2}\right)^2 \left(\frac{h_i + h_{i-1}}{dt}\right)^2 dt}. \quad (3)$$

Validation of the model was made possible in one particular experimental condition with deionized water at 20 °C ± 0.3 °C subcooled condition (80 °C water temperature at atmospheric pressure). Under this condition, bubbles that departed from active cavities were observed to collapse in the subcooled pool near the heated surface (denoted as near field in Fig. 3(a)). Further away from the surface, (between 3 and 5 mm) these bubbles were much smaller size (denoted as far field in Fig. 3(a)). The test section used in this experiment was identical to that shown in Fig. 1(a) and the applied heat flux was 18.94 ± 1.26 W/cm^2. Because of the small (on the order of 10^{-4}) Stokes number of the far-field bubbles, their

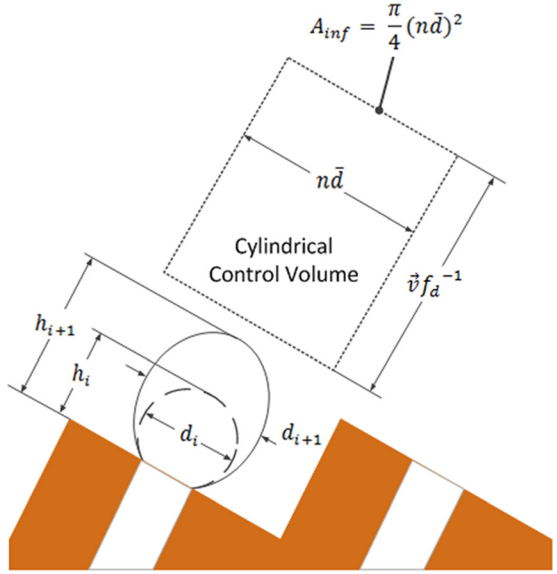

FIG. 2. Schematic of the model indicating bubble growth and the affected liquid volume.

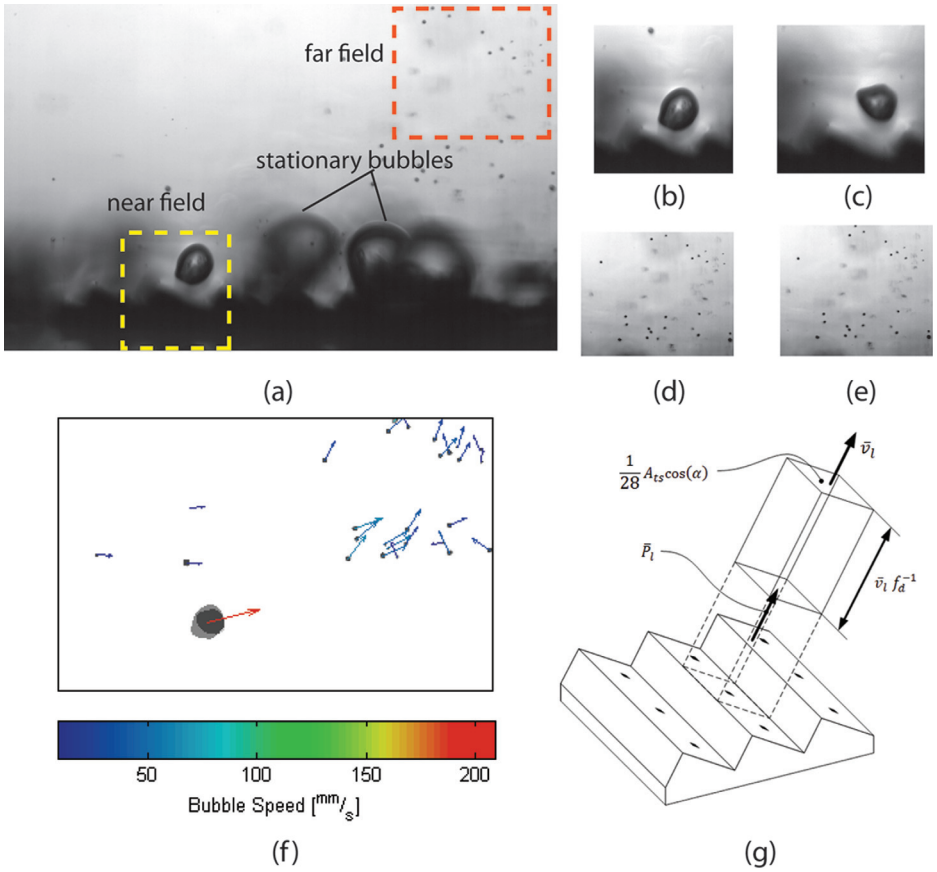

FIG. 3. Subcooled diabatic test results using 20 °C subcooled deionized water for the structured surface shown in Fig. 1(a). (a) Picture from a high speed video showing departing (near-field) bubbles and far field bubbles. Note that the larger bubbles on the right, as in Figs. 1(d) and 1(e), are stationary. Variations in lighting near the surface caused by the temperature and hence density gradients. (b) and (c) Detail of the near field bubbles at two consecutive time intervals 0.3125 ms apart. (d) and (e) Detail of the far field bubbles at two consecutive time intervals 0.3125 ms apart. (f) Bubble tracking velocimetry results indicating a net axial component of flow in the far field as well as a large velocity of the condensing near-field bubble; the average uncertainty in velocity, determined by the errors in estimating bubble displacement, was found to be 3.95%. (g) Control volume of liquid affected by growing bubble from a single cavity. From Kapsenberg *et al.*, in *Proceedings of 13th IEEE Intersociety Conference on ITherm.* Copyright 2012 IEEE. Reprinted by permission of IEEE.[18] (Multimedia view) [URL: http://dx.doi.org/10.1063/1.4871863.3]

settling time was much smaller than the convective time of the bubbles; hence, their velocity is representative of the liquid velocity.[15] Figures 3(b) and 3(c) show two consecutive frames (0.3125 ms apart) of the near field of an active cavity. The bubble is seen to depart normal to the surface and accelerate rapidly during the collapse phase. A custom bubble tracking velocimetry code was developed in Matlab and used to determine the velocity of the far field bubbles.[16] Note that the velocity estimates included an estimation of quantifiable uncertainties due to image distortion by the optics (microscope lens and objective), uncertainty in the image resolution due to uncertainty in the scale of the reference geometry (ratchet pitch) in experiments, and the accuracy in the measurement of that reference geometry.[16,17] Figure 3(f) shows the bubble tracking velocimetry results on the departed bubbles using bubble location information from the frame shown in Fig. 3(a) and its subsequent frame. The near-field departed bubble velocity (Figs. 3(b) and 3(c)) is seen to be in excess of 600 mm/s. In the far field, the bubbles move at a much slower velocity due to the inertia of the quiescent pool (Figs. 3(d) and 3(e)). The velocity of these bubbles, which represents the liquid velocity in the pool, is between 30 and 60 mm/s with a mean component of 25 mm/s parallel to the test surface. The bubbles traveled at this speed and direction for their duration in the field of view. A visual observation during experiments indicated that the plume continued in this direction well outside the camera's field of view. A repeatability experiment was performed 58 days following this experiment and confirmed that the velocity of the plume bubbles were between 30 and 70 mm/s.

The liquid velocity from the experiment was compared against the predicted velocity using the bubble growth model. A slight modification to Eq. (3) was made to account for the area affected by each bubble; the modified control volume of liquid affected by each bubble is shown in Fig. 3(g). Since there were 28 cavities on the test section of footprint A_{ts}, the area of liquid influenced by each active cavity was $(1/28)A_{ts}cos(\alpha)$ in Eq. (3), in place of A_{inf}. The liquid velocity from the bubble growth model is estimated to be 45 mm/s, with a horizontal component of 18 mm/s, which compares reasonably (within 33%) to the velocity of the far-field bubbles from bubble tracking. Given the simplicity of the model this reasonable match with experiments confirms that the bubble growth is largely responsible for the net axial motion imparted to the liquid.

In conclusion, by use of reentrant cavities located preferentially on one slope of mm-sized ratchets, we have demonstrated that liquid motion with a net component parallel to the structured surface can be obtained. A semi-empirical bubble growth model was used to explain the resulting liquid motion using data of bubble growth from high-speed imaging. The concept presented herein can find practical applications in enhanced pool boiling for immersion cooling of electronics as well as in closed-loop passive thermal management systems.

This work was supported in part by the National Science Foundation under Grants 0854503 and 0854132 and in part by the National Aeronautics and Space Administration under Grants NNX09AJ98G and NNX09AL63G.

[1]A. Kosar, C.-J. Kuo, and Y. Peles, Int. J. Heat Mass Transfer **48**, 4867 (2005).
[2]M. C. Chyu and J. Fei, Int. J. Heat Mass Transfer **34**(2), 437 (1991).
[3]S. G. Liter and M. Kaviany, Int. J. Heat Mass Transfer **44**(22), 4287 (2001).
[4]S. H. Bhavnani, G. Fournelle, and R. C. Jaeger, IEEE Trans. Compon. Packag. Technol. **24**(2), 166 (2001).
[5]R. L. Webb, J. Heat Transf. **126**(6), 1051 (2004).
[6]S. G. Kandlikar, Appl. Phys. Lett. **102**(5), 051611 (2013).
[7]H. Linke, B. J. Alemán, L. D. Melling, M. J. Taormina, M. J. Francis, C. C. Dow-Hygelund, V. Narayanan, R. P. Taylor, and A. Stout, Phys. Rev. Lett. **96**, 154502 (2006).
[8]G. Lagubeau, M. Le Merrer, C. Clanet, and D. Quere, Nature Phys. **7**, 395 (2011).
[9]J. Ok, E. Lopez-Ona, D. Nikitopoulos, H. Wong, and S. Park, Microfluid. Nanofluid. **10**(5), 1045 (2011).
[10]G. Dupeux, M. Le Merrer, G. Lagubeau, C. Clanet, S. Hardt, and D. Quere, Europhys. Lett. **96**, 58001 (2011).
[11]N. Thiagarajan, F. Kapsenberg, V. Narayanan, S. H. Bhavnani, and C. D. Ellis, Electron Devices Lett. **33**(7), 1054 (2012).
[12]N. Thiagarajan, "Investigation of thermally-actuated pumping suring pool boiling of a dielectric liquid on an asymmetric microstructured silicon heat sink," Ph.D. dissertation, Auburn University, Auburn, AL, USA, 2013).
[13]V. P. Carey, *Liquid-vapor Phase-change Phenomena: An Introduction to the Thermophysics of Vaporization and Condensation Processes in Heat Transfer Equipment* (Taylor & Francis, London, 1992).
[14]F. M. White, *Fluid Mechanics* (McGraw Hill, New York, 2008).
[15]See supplementary material at http://dx.doi.org/10.1063/1.4871863 for another measure of the liquid velocity using gas injection experiments and particle tracking.
[16]F. Kapsenberg, "Lateral fluid motion in nucleate boiling through asymmetric surface structures," M.S. Thesis, Oregon State University, Corvallis, OR, USA, 2011.
[17]L. Strid, "Passive pumping in pool and open channel configurations via meso-scale asymmetric surface patterning," M.S. Thesis, Oregon State University, Corvallis, OR, 2013.
[18]F. Kapsenberg, N. Thiagarajan, V. Narayanan, and S. H. Bhavnani, in *Proceedings of 13th IEEE Intersociety Conference on ITherm* (San Diego, CA, USA, 2012), pp. 165–175.